Untangling the contribution of adaptive versus non-adaptive processes in the evolution of reproductive isolation between Coenonympha butterflies

Thibaut Capblancq, Camille Roux, Frédéric Boyer, Fabrice Legeai, Mathieu Joron, Laurence Després

Untangling the contribution of adaptive *versus* non-adaptive processes in the evolution of reproductive isolation between *Coenonympha* butterflies.

Thibaut CAPBLANCQ[1,†], Camille ROUX[2], Frédéric BOYER[1], Fabrice LEGEAI[3], Mathieu JORON[4] and Laurence DESPRÉS[1]

[1] *LECA, Université Grenoble-Alpes, Université Savoie Mont Blanc, CNRS, Grenoble, France*

[2] *Univ. Lille, CNRS, UMR 8198 – Eco-Evo-Paleo, F-59000, Lille, France*

[3] *IGEPP, INRAE, Institut Agro, Université de Rennes 1, Le Rheu, France*

[4] *CEFE, Université de Montpellier, CNRS, EPHE, IRD, Montpellier, France*

[†] Corresponding authors:

Thibaut Capblancq, e-mail: thibaut.capblancq@gmail.com

ORCID numbers:

- Thibaut Capblancq (0000-0001-5024-1302)
- Camille Roux (0000-0001-9497-1446)
- Fabrice Legeai (0000-0002-6472-4839)
- Frédéric Boyer (0000-0003-0021-9590)
- Mathieu Joron (0000-0003-1043-4147)
- Laurence Després (0000-0002-0660-6260)

Running title: Evolutionary processes underlying speciation

ABSTRACT

Speciation is a key evolutionary process which has been studied in numerous organisms and at multiple scales, from lineage radiation to gene expression. However, the factors explaining the rise of new species are not yet fully understood, and the relative contribution of neutral *versus* selective evolutionary processes in triggering and maintaining reproductive isolation between lineages is still debated. To explore this question, we study the divergence of two butterfly species, *Coenonympha arcania* and *C. gardetta* (Nymphalidae), which diverged relatively recently but show strong ecological differences. Whole genome sequence data reveal high overall differentiation between the two lineages, best explained by a long period of isolation at the early stage of their divergence. Demographically explicit approaches identify that 6.6% of the genome (32.7 Mbp) is impermeable to gene flow between the two species. Lots of these barrier loci are located on the Z chromosome, potentially spanning 75% of its length which would indicate that a large Z effect is at play in this speciation. Moreover, only a small proportion of barriers showed signatures of selection, suggesting that non-adaptive processes largely contributed to the build-up of reproductive isolation. Therefore, although genes involved in stress response and response to hypoxia are interesting candidates under selection, the adaptation of *C. gardetta* to alpine conditions may not to be the main driver of speciation. Our study brings an original example of intertwined adaptive and non-adaptive processes leading to reproductive isolation in a speciation with secondary contact and improves our understanding of the genomic underpinnings of species divergence.

KEY-WORDS: Demographically explicit models – Genomic barriers – Genomic incompatibilities – Speciation genomics – Z chromosome

INTRODUCTION

The extensive array of living organisms emerges from a fundamental process in evolution: speciation. In the 20th century, this process was regarded as a series of binary divisions in evolutionary lineages, primarily depicted through phylogenetic trees. While this dichotomous perspective upholds the evolutionary connections between groups, its significance diminishes when lineages are closely related. Hence, speciation is now well accepted as a continuous process, gradually giving rise to distinct entities and eventually species (Stankowski & Ravinet, 2021). The accumulation of mutations in the genomes progressively results in the isolation of the two lineages by reducing the fitness of their hybrids (Presgraves, 2010). Within the whole range of substitutions between two species, only some affect hybrid fitness, either by generating incompatibilities in gene interactions (*i.e.*, endogenous postzygotic isolation), by being involved in ecological adaptations (*i.e.*, exogeneous postzygotic isolation) or in mating signals (*i.e.*, prezygotic isolation) (Coyne & Orr, 2004). The relative importance of these different types of hybrid incompatibility on the evolution of reproductive isolation varies depending on the demographic and ecological contexts of the speciation event.

Identifying the evolutionary processes that led to the establishment of such barriers between closely related lineages is critical for understanding the emergence of new species (Seehausen *et al.*, 2014). Their nature can be broadly classified according to whether they originated through adaptive or non-adaptive processes. Non-adaptive forces lead to the formation of barriers when interacting genes co-evolve differently within isolated lineages. Negative interactions between these co-evolving loci have been shown to be commonly expressed in hybrids, leading to strong reproductive barriers (Bateson, 1909; Dobzhansky, 1936; Muller, 1942). In such case, the formation of hybrids leads to the expression of new interactions that have not been proven by natural selection (Simon *et al.*, 2018). Each set of co-evolving deleterious and compensatory mutations can thus become a potential endogenous

barrier, impacting the hybrid fitness regardless of the ecological context in which the parent species evolved. Conversely, adaptive processes involve loci whose genotype fitness is directly dependent on the environment. In that case, hybrids tend to be less fit than one of the two parents, depending on the environment in which they are located (Schluter, 2009). The relative importance of the above mentioned non-adaptive and adaptive processes in the build-up of reproductive isolation is tightly linked to the demographic and ecological contexts in which the speciation takes place. In sympatry with environmental heterogeneity, the predominant drivers of barriers are adaptive processes and exogeneous selection (Nosil, 2012), while in allopatry endogenous barriers may arise as a result of genetic drift (Endler, 1977; Barton & Hewitt, 1985; Noor & Bennett, 2009).

To investigate empirically the comparative influences of adaptive and non-adaptive processes on reproductive isolation, it is essential first to pinpoint the genomic regions linked to these barriers, the so-called "barrier loci" (Roux *et al.*, 2016; Ravinet *et al.*, 2017). This step allows analyzing the evolutionary forces that have influenced their recent history. Identifying species barriers *in natura* can be achieved when a pair of closely related species are experiencing gene flow, either as a result of secondary contact, or continuously during their divergence process (Smadja & Butlin, 2011; Martin *et al.*, 2013). If strong selection acts against migrant alleles in specific genomic barriers while the rest of the genome is exchanged more freely between species, then patterns of nucleotide polymorphism and divergence may be sufficiently contrasted to detect barrier loci (Fraïsse *et al.*, 2021; Laetsch *et al.*, 2023). In that spirit, new methodological developments have taken advantage of large genomic and computational resources to test a local reduction in migration rate using window-based approaches. Two methods have recently been distributed to carry out genomic scans of species barriers: gIMble (Laetsch *et al.*, 2023) and DILS (Fraïsse *et al.*, 2021). These methods have the advantage to account for the confounding effect of background selection,

which can produce differentiation patterns similar to those of divergent selection (Charlesworth *et al.*, 1997; Cruickshank & Hahn, 2014). Background selection results in a local reduction of genetic diversity due to purifying selection against deleterious mutations, and promotes high species differentiation without playing a functional role in reproductive isolation (Charlesworth, 2012). The two above mentioned approaches tackle this issue and show great potential to identify genomic regions involved in reproductive isolation. The identification of such barriers stands as a prerequisite to unravel the evolutionary mechanisms determining their evolution. For instance, contrasting the genomic patterns of polymorphism and divergence within these barrier regions against the broader genomic background allows testing whether they are predominantly shaped by local adaptive processes or not (McDonald & Kreitman, 1991; Stoletzki & Eyre-Walker, 2011; Han *et al.*, 2017; Irwin *et al.*, 2018; Shang *et al.*, 2021; Moreira *et al.*, 2023).

In this study we dissect the genetic architecture of reproductive isolation between two temperate butterflies, *Coenonympha arcania* and *C. gardetta*, and estimate the relative contributions of adaptive *versus* non-adaptive processes to their speciation. The two species are ecologically divergent, with *C. arcania* being widely distributed in Europe, from sea level to elevations around 1,500 meters, while *C. gardetta* is typically encountered in subalpine and alpine habitats, above 1,500 meters in the Alps. They diverged around 1.7 million years ago (Capblancq *et al.*, 2015), are morphologically distinct and have parapatric distributions with multiple contact zones at intermediate elevation around the Alps. The two species do not form two distinct monophyletic groups based on mtDNA, which suggests that mitochondrial transfers (and gene flow) occurred sometime during their divergence (Capblancq, 2016). Occasional hybrids between the two species can be observed in regions of sympatry (Capblancq *et al.*, 2019), confirming a potential for ongoing gene flow, although they would supposedly be unfit or mostly sterile according to previous experimental crosses (de Lesse,

1960). This strong but incomplete reproductive isolation makes the species pair an ideal model to study the genomics of speciation and identify barrier loci along the species genome. In presence of gene flow, if ecological divergence is the main driver of speciation (i.e., ecological speciation), loci involved in local adaptation and reproductive isolation should be largely shared. Conversely, if reproductive isolation evolved independently from local adaptation, signatures of restricted gene flow should not be necessarily associated with signature of selection.

To explore these questions, we surveyed whole genomes from natural populations of the two species with four main objectives: 1) study the temporal patterns of gene flow between *C. arcania* and *C. gardetta* (*i.e.*, isolation *versus* continuous migration *versus* secondary contact *versus* ancestral migration), 2) locate barrier loci where gene flow is effectively blocked, 3) evaluate the relative importance of adaptive *versus* non-adaptive processes in determining reproductive isolation, and 4) identify candidate speciation genes. To achieve this, we generated whole-genome short read data for 19 individuals of *C. arcania* and 17 individuals of *C. gardetta* and mapped the sequences to the *C. arcania* reference genome (Legeai *et al.*, 2024). We then explored genetic diversity and differentiation along the genome of the species using 50kbp windows and located genomic regions displaying reduced gene flow (referred to as "barrier loci") using both gIMble and DILS. We then sought signatures of selection both within and outside these barrier regions, in order to qualify the forces shaping the observed variation in gene flow levels along the genome.

RESULTS

A total of 65.2 million cleaned reads were obtained on average per individual (range: 46.6-88.5 million reads), of which 54.5% mapped to the *C. arcania* reference with a quality score equals or above 20. After removal of PCR duplicates, mean coverage across all individuals

was 18x (range: 13-25.2x), and genotype likelihoods were obtained for 203,075,624 sites that passed quality and coverage thresholds for both species, scattered across 9,844 50kb genomic windows representing 99% of the reference genome length (497Mbp, Legeai *et al.*, 2024). Among these sites, 16,571,294 were polymorphic (8.2% of the covered sites) and were homogeneously distributed along the 30 first large scaffolds of the reference (Supplemental Fig. S1).

Demographic inferences favor a scenario of secondary contact and low levels of gene flow between species

To investigate the history of divergence and gene flow between *C. arcania* and *C. gardetta* we compared the likelihood of four speciation scenarios: strict isolation (SI), isolation with migration (IM), secondary contact (SC) and ancient migration (AM), using Fastsimcoal2 (Excoffier *et al.*, 2013) and DILS (Fraïsse *et al.*, 2021). We used the whole dataset for demographic inferences because including or not the sexual chromosome Z gave very similar results (Supplemental Table S1).

Both procedures favored a model of isolation followed by a secondary contact for the divergence of *C. arcania* and *C. gardetta* (Figure 1), in contrast with previous results that favored an isolation with migration scenario (Capblancq *et al.*, 2019), but confirming the presence of gene flow during the speciation process. The initial divergence time estimates were very similar for the two methods with Fastsimcoal2 inferring 1.79 Mya and DILS inferring 1.93 Mya (Figure 1). The secondary contact would have occurred only after a relatively long period of isolation, 360,240 generations ago according to Fastsimcoal2 and 498,562 generations ago according to DILS. The migration rate estimated after the secondary contact between the two species was low (Fastsimcoal2: $m_{e\ \text{arc-gar}}$ = 9.07e-8, $m_{e\ \text{gar-arc}}$ = 3.99e-7; DILS: $m_{e\ \text{arc-gar}}$ = 2.9e-7, $m_{e\ \text{gar-arc}}$ = 7.9e-7), roughly corresponding to an exchange of 0.5 to 1.5 individuals every generation. Finally, the current N_e estimates inferred were 2,955,432

(Fastsimcoal2) or 2,659,735 (DILS) for *C. arcania* and 1,748,050 (Fastsimcoal2) or 1,257,299 (DILS) for *C. gardetta*, this time very much consistent with previous estimates inferred from ddRAD-seq data (Capblancq *et al.*, 2019).

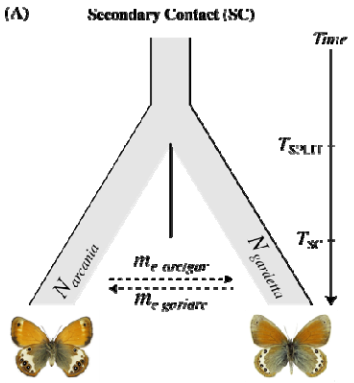

(B)

	Fastsimcoal (95% CI)		DILS (95% CI)	
Best scenario	**SC**	Δ_{AIC} AM = 311,210 Δ_{AIC} IM = 302,806 Δ_{AIC} SI = 3,980,332	**SC**	proba migration = 0.982 proba SC vs IM = 0.903
Divergence times				
T_{SPLIT}	1,793,459 *(1,694,115 - 1,892,802)*		1,930,105 *(1,688,758 - 2,182,893)*	
T_{SC}	360,240 *(293,122 - 427,358)*		498,562 *(381,457 - 602,492)*	
Effective sizes				
N arcania	2,955,432 *(2,913,267 - 2,997,597)*		2,659,735 *(2,296,304 - 3,189,278)*	
N gardetta	1,748,050 *(1,737,751 - 1,758,348)*		1,257,299 *(795,278 - 1,857,227)*	
Migration rates				
m_e arc/gar	3.99e-07 *(0 - 1.2e-05)*		7.9e-07 *(6.37e-07 - 9.29e-07)*	
m_e gar/arc	9.07e-08 *(0 - 1.2e-04)*		2.9e-07 *(1.87e-07 - 4.33e-07)*	

Figure 1: Scenario of divergence between *C. arcania* and *C. gardetta*. (A) Most likely scenario of divergence with its associated parameters. (B) results of Fastsimcoal2 and DILS inferences with the most likely model (SC) in comparison with the three other tested scenarios of divergence (AM, IM and SI) and the inferred parameter values. 95% confidence intervals are shown in brackets.

Identifying genomic barriers to gene flow unravels the importance of the Z chromosome and several autosomal regions

To locate putative barrier loci, we used two recently published model-based approaches that test for a local reduction of migration along the chromosome of two diverging species: an adaptation of gIMble (Laetsch *et al.*, 2023) – the Δ_B method – and DILS (Fraïsse *et al.*, 2021). Both approaches follow a very similar process that does not contrast different genomic regions among each other, but two demographic models (with or without gene flow) within each genomic window. The gene flow *vs* no gene flow comparison is made at the window level specifically to account for the variation in local effective population sizes along the genome, variation that can originate from evolutionary factors (linked selection) or be due to intrinsic parameters (reduced recombination rates). The two methods identified 654 genomic regions acting as barrier to gene flow between the genomes of *C. arcania* and *gardetta*, representing 6.6% of the genome. These regions were mostly located on the sex chromosome

Z (363 windows = 56% of the barriers) but also on multiple autosomal regions of high genetic differentiation (Figure 2A). The Δ_B method returned 6.5% of the genome as barrier to gene flow, with almost the entire Z chromosome (74.7%), suggesting that the very high F_{ST} and low diversity estimates along this sex chromosome (Supplemental Fig. S2) were not only due to its reduced effective size (3/4 of autosomal N_e). We also tried a migration rate threshold inferred only with the Z chromosome to estimate the Δ_B. The procedure still returned multiple barrier loci in the Z chromosome but only representing 8.6% of its length (Supplemental Fig. S3). False Positive Rate (FPR) estimated at the window level using simulations was zero for most genomic regions, and only 40 windows returned a non-zero FPR of 1%, supporting the robustness of the procedure. DILS, which, in general, identified a reduced number of barriers compared to the Δ_B method (only 0.3% of the genome), also found nearly half of the barriers (11/27 windows) on the Z chromosome (Figure 2A). The substantial difference between the number of regions identified as barrier by the Δ_B method (642 windows) and DILS (27 windows) was somewhat surprising, with only 15 common windows. This calls for further comparisons of the procedures in the future. Hereafter, we considered as barriers all 654 windows that were identified by either one or the other method, or both. Generally, these windows were localized in genomic regions of increased genetic differentiation and low diversity, but not always (*e.g.*, on chromosome 2, 10 or 12), confirming that genetic differentiation and resistance to gene flow may not always be associated.

Patterns of differentiation (F_{ST}), divergence (d_{XY}), and diversity (π) along the two species genomes were also investigated to locate "genomic islands" in the genomic landscape. The procedure of Shang et al (2021) was used, which allows to distinguish three scenarios of selection (recurrent, divergent, balancing) from a neutral signal by identifying extreme combinations of π, d_{XY} and F_{ST}. Only genomic regions putatively under recurrent

selection or balancing selection were identified (Figure 2B). The recurrent selection loci, which showed extremely high values of F_{ST}, low values of π and average values of d_{XY}, were found in multiple autosomal regions and the Z chromosome. Recurrent selection corresponds to a selective pressure that is acting on the two diverging lineages and was already operating in the ancestral population. The 24 genomic regions located within barriers and identified as under recurrent selection (circled points in Figure 3B) constituted the genomic window "linked to barrier and with signals of positive selection" set for downstream analyses. One of these regions was located on the Z chromosome and the rest distributed on nine of the 29 autosomes.

Zooming in on these candidate regions often allowed to identify peaks or "islands" in the genomic landscape (Figure 2C). As expected, the candidate regions showed elevated F_{ST} and decreased genetic diversity, but they also returned elevated values of DoS (Direction of Selection) in coding regions, suggesting more positive selection than in the rest of the genome. For example, a peak of high DoS values (>> 0) was observed in the middle of chromosome 15 (Figure 2C), a genomic region identified as a barrier to gene flow and exhibiting increased genetic differentiation between and depleted diversity within the two species. However, when DoS is examined gene by gene along the genome, identifying a specific pattern was difficult and many genes with very high DoS values were found in genomic regions not identified as potential barriers or not showing any specific genetic diversity or differentiation (Supplemental Fig. S4).

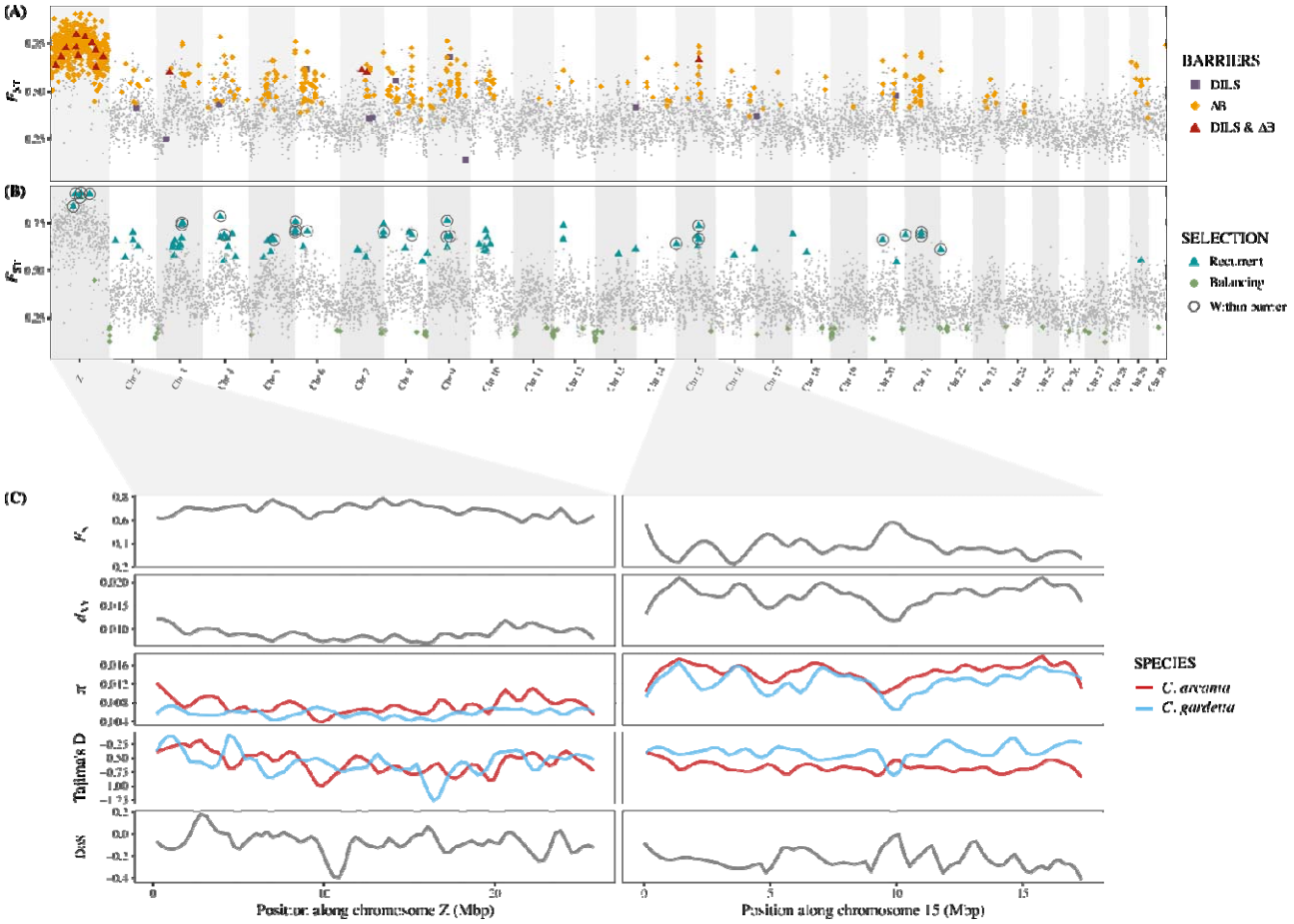

Figure 2: Identification of barriers to gene flow between the genomes of *C. arcania* and *C. gardetta*. (A) Genomic windows considered as resistant to gene flow using two process-based procedures: the ΔB procedure ($\Delta B > 0$) and/or DILS (posterior probability of being a barrier > 0.7). (B) Windows falling into one of the four selection scenarios described in (Shang *et al.*, 2021) based on extreme patterns of F_{ST}, d_{XY} and π. (C) Zoom on chromosome Z and 15 showing different genetic parameters for each genomic window and species. Barriers detected with both DILS and Δ_B approaches are localized with shaded grey rectangles.

Can we disentangle the evolutionary processes shaping heterogenous genomic resistance to gene flow?

To better understand the evolutionary forces that shaped the landscape of genetic diversity within and differentiation between *C. arcania* and *C. gardetta*, multiple genetic parameters were inspected across 9,844 genomic windows on the Z chromosome and the autosomes. As expected, the Z chromosome showed different patterns compared to autosomes (Figure 3, Supplemental Fig. S2), with an F_{ST} almost twice as high on Z than on autosomes ($F_{ST(Z)}$ =

0.687; $F_{ST(A)}$ = 0.357), a much lower net divergence ($d_{a(Z)}$ = 0.0024; $d_{a(A)}$ = 0.0038), nucleotide diversity twice as low in both species ($\pi_{(Z)arcania}$ = 0.0074; $\pi_{(A)arcania}$ = 0.0145; $\pi_{(Z)gardetta}$ = 0.0058; $\pi_{(A)gardetta}$ = 0.0131), a much higher DoS on average ($DoS_{(Z)}$ = -0.033; $DoS_{(A)}$ = -0.201) and a lower density of genes. Tajima's *D* values were similar on the sex chromosome (Tajima's $D_{(Z)arcania}$ = -0.58; Tajima's $D_{(Z)gardetta}$ = -0.58) but the alpine specialist showed larger estimates on the autosomes (Tajima's $D_{(Z)arcania}$ = -0.65; Tajima's $D_{(Z)gardetta}$ = -0.36). In a similar trend, the genomic windows identified as barriers showed higher differentiation ($F_{ST(barrier)}$ = 0.63; $F_{ST(no\ barrier)}$ = 0.37), lower net divergence ($d_{a(barrier)}$ = 0.0031; $d_{a(no\ barrier)}$ = 0.0038), higher signal of positive selection ($DoS_{(barrier)}$ = -0.017; $DoS_{(no\ barrier)}$ = -0.196) and lower genetic diversities ($\pi_{(barrier)arcania}$ = 0.0097; $\pi_{(no\ barrier)arcania}$ = 0.0143; $\pi_{(barrier)gardetta}$ = 0.0076; $\pi_{(no\ barrier)gardetta}$ = 0.0128).

Four categories of genomic regions were distinguished. The genomic windows identified as barriers were distinguished from the non-barrier windows and, within each of these two categories, windows showing signals of positive selection (*i.e.*, recurrent selection in Figure 2) were distinguished from the windows showing no signals of selection. The four resulting types of windows were: i) unlinked to barrier and without signal of positive selection, ii) unlinked to barrier but with signals of positive selection, iii) linked to barrier without positive selection and iv) linked to barrier with positive selection. Among the windows showing no signal of positive selection, net divergence (d_a), gene density and Tajima's D were similar within and outside barriers, whereas a higher genetic differentiation (F_{ST}), larger DoS and lower autosomal nucleotide diversity (π) were found in windows linked to barriers compared to those outside barriers (Figure 3). Windows with signals of positive selection, linked or not to barriers, showed increased F_{ST}, lower d_a, π and Tajima's D compared to regions with no positive selection, but also a higher density of genes. Significantly higher values of F_{ST} (t-test: *p-value* = 3.9e-06) and DoS (t-test: *p-value* = 0.014)

were found in windows linked to barriers compared to non-barrier regions when positive selection was identified (Figure 3). However, genomic windows linked to barriers but without selection were not significantly different than regions unlinked to barriers in terms of d_a, DoS or gene density, confirming that their resistance to interspecific gene flow was not linked to undetected positive selection. In the same vein, linkage disequilibrium (LD) was much higher in barriers with positive selection than in the other three categories, consistent with hitchhiking effects. On the contrary, barrier regions with no signal of positive selection returned LD values comparable to non-barrier windows, suggesting little linked selection.

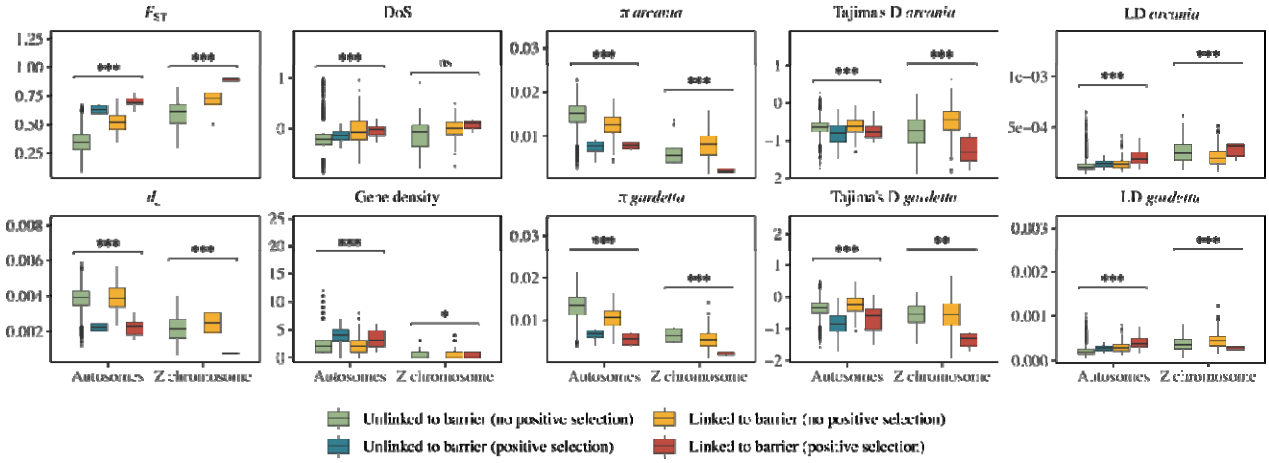

Figure 3: Distribution of genomic parameters in autosomes and chromosome Z, within or outside barrier loci and within or outside windows under positive selection. Are considered barrier loci here all the genomic windows that returned a $\Delta_B > 0$ and/or a DILS posterior probability > 0.7 and fell in one of the genomic islands identified in Figure 2(A). Student's t-tests returned extremely significant results (*p-value* < 0.001) between the Z chromosome and the autosomes for all parameters. One-way ANOVA tests with the four categories as grouping factor were conducted independently for the Z chromosome and the autosomes for each genomic parameter: a *p-value* < 0.001 is indicated by '***', *p-value* < 0.01 by '**', *p-value* < 0.05 by '*' and 'ns' for a *p-value* > 0.05.

Finally, to avoid a loss of information associated with averaging gene-level information across 50kb genomic window we complemented our analysis with a gene centered approach, by looking at the proportion of genes showing a positive DoS in the four previously described categories (Table 1). Overall, 8.4% of the 15,239 analyzed genes returned a DoS > 0. Windows unlinked to barriers and showing no positive selection were

296 depleted in positive DoS, suggesting a major role of purifying selection in these regions. On
297 the contrary, windows unlinked to barriers but showing signals of selection showed higher
298 values of DoS, presumably because directional selection counteracted purifying selection in
299 these regions. Genomic regions associated with barriers returned an overall inflated
300 proportion of genes with positive DoS and hosted very few genes with extremely low DoS
301 value (< –0.5). This confirmed that the patterns observed for DoS on Figure 3 were not due to
302 a few high DoS outlier genes in windows linked to barriers, but to a more general trend in
303 these regions.

Barrier	Selection	Nb of genes	DoS > 0	DoS < -0.5
Unlinked to barrier	No positive selection	14,255	6.7%	11%
	Positive selection	152	21%	6%
Linked to barrier	No positive selection	726	36.8%	1.7%
	Positive selection	57	40.4%	6.4%

304

305 **Table 1:** Proportion of genes returning positive (>0) or a very negative (<-0.5) value of Direction of
306 Selection (DoS) within the four different types of genomic windows identified in the study.

307 *The genes of reproductive isolation (?)*

308 To explore the potential differences in gene functions within the two types of barriers (with
309 or without signal of positive selection), a gene ontology (GO) terms enrichment analysis was
310 conducted for each group. Significantly enriched GO terms were largely shared between the
311 barriers showing signals of positive selection and those showing no such signals (Figure 4).
312 These shared terms included one term associated with energy production: “electron transport
313 chain”, two linked to development: “cell morphogenesis” and “axon guidance”, and another
314 two associated with lipid production: “phospholipid metabolic process” and “lipid
315 biosynthetic process”. One biological process enriched only in barriers with no signals of
316 selection was linked to “sensory perception of smell”, suggesting incompatibilities in the
317 olfactive systems of the two species, without selection acting within or between species. On
318 the contrary, one biological process significantly enriched only in barriers showing signals of

positive selection was associated with methylation. The Z chromosome was initially considered separately from the autosomes in the GO terms enrichment analysis, but only one biological process was slightly significantly enriched in the barrier windows of the sex chromosome: “regulation of catalytic activity”; this means that all the processes showing enrichment in barrier windows (Figure 4) are mostly driven by enrichment in autosomal barriers.

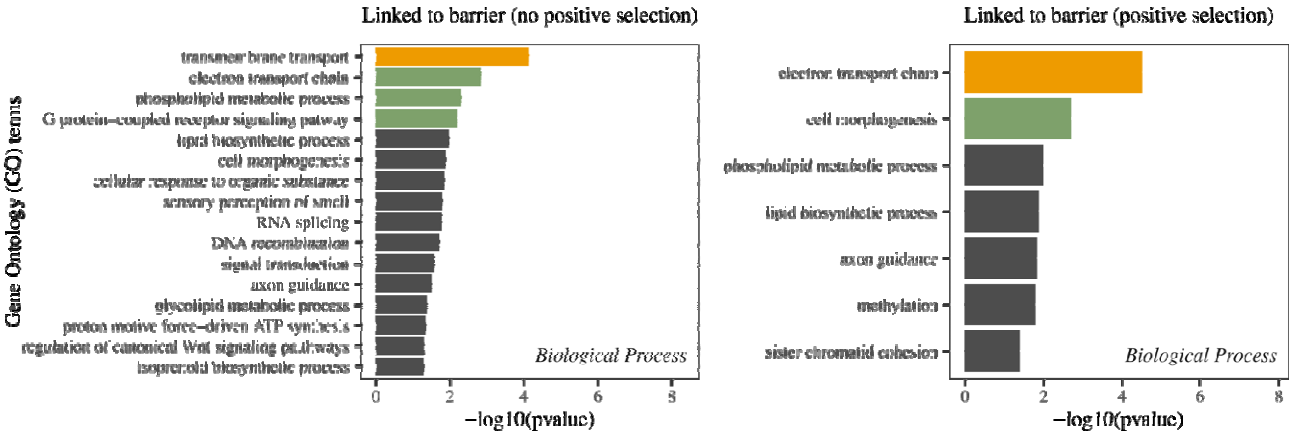

Figure 4: Results of the GO terms enrichment in the genomic regions identified as putative barrier loci between *C. arcania* and *C. gardetta* (both with and without signals of positive selection), with the associated biological processes. Only GO terms found significantly enriched with a Kolmogorov Smirnov test are shown (*p-value* < 0.05) and GO terms shown in green and yellow have strongly significant test results, *p-value* < 0.01 and < 0.001, respectively.

We then inspected the genes located within genomic barriers that also showed signals of positive selection, hypothesizing that they were the ones driving reproductive isolation between *C. arcania* and *gardetta*. In these windows, we found many genes linked to response to stress and especially hypoxia in other species, including those encoding serine/threonine protein kinases, apoptosis-inducing factors, phosphatidylserine synthases or fatty acid synthetases (Table 2).

Chromosome	Gene ID	Putative protein	Reference
Z	CARC000666	forkhead box protein F1 A like	*Pararge aegeria*
	CARC000760	protein RCC2	*Maniola hyperantus*
Chr 3	CARC014850	alpha N-terminal protein methyltransferase 1-like	*Maniola jurtina*
	CARC014851	golgin subfamily A member 2	*Maniola hyperantus*
	CARC014852	WD repeat-containing protein 82	*Maniola hyperantus*
	CARC014853	chromodomain-helicase-DNA-binding protein 7	*Pararge aegeria*
	CARC014854	chromodomain-helicase-DNA-binding protein 7	*Maniola jurtina*
	CARC014855	probable NADH dehydrogenase [ubiquinone] iron-sulfur protein 6	*Maniola jurtina*
	CARC015230	UPF0184 protein AAEL002161	*Bicyclus anynana*
	CARC015231	phosphatidylserine synthase 1	*Maniola hyperantus*
	CARC015232	phosphatidylserine synthase 1	*Maniola hyperantus*
	CARC015233	transmembrane protein 189	*Bicyclus anynana*
Chr 4	CARC016321	structural maintenance of chromosomes protein 6	*Maniola jurtina*
	CARC016372	decapping nuclease DXO homolog	*Maniola jurtina*
	CARC016373	zinc finger protein 91-like	*Maniola jurtina*
	CARC016374	exostosin-3	*Bicyclus anynana*
	CARC016375	exostosin-3	*Bicyclus anynana*
	CARC016376	glycosyl transferase family 64 domain-containing protein	*Phthorimaea operculella*
	CARC016975	GRIP and coiled-coil domain-containing protein 2	*Pararge aegeria*
Chr 5	CARC017771	nucleosome-remodeling factor subunit NURF301	*Maniola jurtina*
Chr 6	CARC018005	mRNA export factor	*Maniola hyperantus*
	CARC018009	low-density lipoprotein receptor-related protein 1	*Pararge aegeria*
	CARC018010	low-density lipoprotein receptor-related protein 1	*Pararge aegeria*
	CARC018011	low-density lipoprotein receptor-related protein 1	*Maniola jurtina*
	CARC018012	platelet endothelial aggregation receptor 1	*Vanessa atalanta*
	CARC018133	eukaryotic translation initiation factor 2 subunit 1	*Maniola hyperantus*
	CARC018134	probable phenylalanine--tRNA ligase	*Maniola jurtina*
	CARC018790	endonuclease G, mitochondrial	*Maniola hyperantus*
	CARC018921	SOSS complex subunit B homolog	*Maniola jurtina*
Chr 7	CARC019260	eukaryotic translation initiation factor 4 gamma 2-like	*Maniola hyperantus*
	CARC019261	MOB kinase activator-like 2	*Aricia agestis*
	CARC019262	MOB kinase activator-like 2	*Pararge aegeria*
	CARC019263	palmitoyltransferase Hip14	*Maniola jurtina*
Chr 8	CARC019863	elongation of very long chain fatty acids protein	*Maniola jurtina*
	CARC020154	probable tRNA N6 adenosine threonylcarbamoyltransferase	*Maniola hyperantus*
	CARC020155	traB domain-containing protein-like	*Maniola hyperantus*
	CARC020156	traB domain-containing protein-like	*Pararge aegeria*
	CARC020157	formylglycine-generating enzyme	*Maniola jurtina*
Chr 9	CARC020673	glucose dehydrogenase [FAD, quinone]	*Bicyclus anynana*
	CARC020674	glucose dehydrogenase [FAD, quinone]	*Maniola jurtina*
	CARC020714	oxysterol-binding protein 1	*Maniola jurtina*
	CARC021113	apoptosis-inducing factor 3	*Maniola hyperantus*
Chr 15	CARC004770	fatty acid synthase	*Maniola jurtina*
	CARC004961	leukocyte receptor cluster member 1 homolog	*Maniola jurtina*
	CARC004962	peroxisomal membrane protein PMP34	*Bicyclus anynana*
	CARC005274	WASH complex subunit 5	*Pararge aegeria*
	CARC005275	WASH complex subunit 5	*Pararge aegeria*
	CARC005277	protein SCAF11	*Maniola jurtina*
Chr 20	CARC009021	DNA polymerase alpha subunit B	*Maniola jurtina*
	CARC009424	mitochondrial amidoxime-reducing component 1-like	*Pararge aegeria*
	CARC009425	mitochondrial amidoxime reducing component 2-like	*Maniola jurtina*
Chr 21	CARC009609	NADH dehydrogenase [ubiquinone] iron-sulfur protein 3	*Maniola jurtina*
	CARC009610	serine/threonine-protein kinase TBK1	*Maniola jurtina*
	CARC009782	anaphase-promoting complex subunit 6-like	*Pararge aegeria*
	CARC009783	retinalized-like protein 2	*Maniola hyperantus*
	CARC009784	hypothetical protein EVAR_21052_1	*Eumeta japonica*
	CARC009785	RNA polymerase II subunit A C-terminal domain phosphatase	*Maniola jurtina*
	CARC010101	endoplasmic reticulum metallopeptidase 1-like	*Maniola hyperantus*
	CARC010004	guanine nucleotide-binding protein subunit beta-5	*Aricia agestis*
	CARC010005	neuroplastin	*Melitaea cinxia*
	CARC010006	pachytene checkpoint protein 2	*Maniola jurtina*
	CARC010199	proton-coupled amino acid transporter-like protein CG11139	*Maniola jurtina*
	CARC010200	peroxisomal membrane protein 11B	*Maniola hyperantus*
	CARC010202	RNA-binding protein spenito	*Pararge aegeria*
	CARC010203	leukotriene A-4 hydrolase	*Maniola jurtina*
	CARC010204	39S ribosomal protein L13, mitochondrial	*Maniola hyperantus*
	CARC010352	cactin	*Maniola jurtina*
	CARC010353	tudor domain-containing protein 5	*Vanessa cardui*

Table 2: List of the 68 protein-coding genes annotated within the genomic windows identified as barrier loci between *C. arcania* and *C. gardetta* and showing signals of positive selection. The table includes gene IDs, a description of the associated protein functions and the reference organism for which the highest homology was found by Diamond v2.0.13 on NCBI NR 2022-11-30.

DISCUSSION

When studying divergence between closely related species showing strong ecological divergence in close geographic proximity (*i.e.*, sympatry or parapatry), it is tempting to hypothesize that speciation is mainly driven by divergent selection (Schluter, 2009). Examples showing a large impact of environmental drivers on the speciation process are indeed growing in the literature (Nosil, 2012). However, in more cases than anticipated, the initiation of speciation appears to be linked to non-adaptive intrinsic barriers, even for ecologically divergent species pairs (Presgraves, 2010). Our results show that most genomic regions resisting gene flow between *C. arcania* and *C. gardetta* are not under positive selection, even though signatures of selection, putatively linked to the adaptation of *C. gardetta* to high elevation, can be found in a small proportion of them. The precise contribution of neutral *versus* adaptive processes on the evolution of reproductive isolation is difficult to estimate without knowing the size effect of the genes involved. However, the large proportion of barrier loci with no signal of positive selection suggests that the build-up of reproductive isolation between the ecologically divergent *C. arcania* and *C. gardetta* was largely influenced by intrinsic non-adaptive barriers.

Divergence with gene flow but mostly isolation

The demographic context of a speciation event, and especially the extent and continuity of gene flow between the diverging populations, can strongly influence the processes initiating or maintaining reproductive isolation. A secondary contact scenario between *C. arcania* and *C. gardetta* appears likely, with putatively strong isolation during the initial stage of the speciation process. The split between the ancestral populations of *C. arcania* and *C. gardetta* would have happened at the beginning of the Pleistocene around 1.8 million years ago, in agreement with previous estimates (Kodandaramaiah & Wahlberg, 2009; Capblancq *et al.*,

366 2015). This geological period is known to be associated with climate cooling and with an
367 increase in speciation events (Levsen *et al.*, 2012; April *et al.*, 2013; Nevado *et al.*, 2018). At
368 that time, a fraction of the species' ancestral population likely became isolated and gave birth
369 to the current *C. gardetta* lineage. Our results also confirmed the presence of gene flow
370 during the speciation of *C. arcania* and *C. gardetta*, since a secondary contact ~400,000
371 generations ago. However, migration between the two species is relatively recent and at low
372 frequency with only a few effective individuals per generation (0.5 – 1.56). While these
373 numbers are comparable with other hybridizing butterfly species with similar divergence time
374 such as *Heliconius melpomene* and *cydno* (Martin *et al.*, 2015), they usually correspond to
375 species pairs that have experienced gene flow all along their divergence process, and thus
376 much more cumulative migration throughout their speciation. It is therefore difficult to assess
377 how much migration is associated with effective gene flow between *C. arcania* and *C.*
378 *gardetta*, especially knowing that mostly F1 hybrids are observed in places where the two
379 species co-occur (Capblancq *et al.*, 2019).

380 The genomics of speciation have been largely studied in pairs of species for which the
381 speciation scenario involves gene flow all along the divergence process (Feder *et al.*, 2012).
382 A pure isolation with migration (IM) scenario is nonetheless unlikely for a lot of hybridizing
383 temperate species, which often encompassed period of strict isolation due to large range
384 shifts associated with climate fluctuations (De Jode *et al.*, 2023). This *Coenonympha* species
385 pair is one example where migration was interrupted during a large part of the speciation
386 process. In these circumstances, homogenizing gene flow was probably not strong (and/or
387 continuous) enough to lower differentiation at neutral genomic regions in comparison with
388 divergently selected regions, only slightly affecting the genomic landscape of the two species.
389 This pushed us to go beyond the search for contrasts in genetic diversity and differentiation

that is widely used in the literature (Turner *et al.*, 2005; Nosil *et al.*, 2009), to identify the genomic bases of speciation in our species pair.

Locating the genomic regions contributing to reproductive isolation

The use of process-based procedures was decisive to distinguish the genomic regions involved in reproductive isolation from the regions pervasive to gene flow. The principle behind these methods is relatively simple: scanning the genome of two hybridizing species in search for regions resisting gene flow (Fraïsse *et al.*, 2021; Laetsch *et al.*, 2023). Recently published procedures use demographically explicit models to test the superiority of a scenario without gene flow over one allowing migration, at the genomic window level. We compared the outcome of two of these methods: DILS, developed by Fraïsse and colleagues (2021) and an adaptation of gIMble, developed by Laetsch and colleagues (2023): the Δ_B method. The two procedures identified multiple regions acting as barriers between *C arcania* and *C. gardetta*, with one large barrier on the Z chromosome and the rest distributed on nine of the 29 autosomes. These were not necessarily located within genomic windows showing extreme patterns of genetic diversity and differentiation. Nonetheless, the results of DILS and Δ_B are not totally concordant, except for the strong signal on the Z chromosome. It could suggest a different sensitivity of the two methods to the overall heterogeneity of gene flow and/or effective population sizes, or variation in their stringency. It is important to note that we analyzed the Z chromosome together with the autosomes here, which is sometimes avoided in the literature (Laetsch *et al.*, 2023). While the lower effective population size of the Z chromosome is accounted for in this type of procedure, which re-infer local diversity at the genomic window level, differences in migration rates between the sex chromosomes and the autosomes (e.g., sex-biased migration) could lead to erroneous results. We are not aware of such context in *Coenonympha* butterflies but we need to keep in mind that it could greatly lower the number of barrier loci identified on the Z chromosome (Supplemental Fig. S3).

Exploring the genomic landscape of diversity within and differentiation between species also provided important information. Tajima's *D*, for example, was low on average but show extreme troughs of negative values at multiple restricted genomic regions. Extremely negative values of Tajima's *D* imply a recent and strong increase of low frequency alleles, which, when forming a peak in a specific genomic location, is usually linked to a recent selective sweep (Carlson *et al.*, 2005). We observed multiple valleys of very low Tajima's *D* in *C. gardetta* population. They likely originated in response to the selection of alleles allowing the species adaptation to alpine-like environment during the speciation process. Within or close to these Tajima's *D* troughs we also found signals of recurrent selection, which refers to a scenario where a selective pressure that already acted on the ancestral population still acts on the diverging lineages, reducing polymorphisms within and net divergence between species while increasing differentiation (Han *et al.*, 2017; Irwin *et al.*, 2018; Shang *et al.*, 2021). Therefore, genes important for adaptation, both within and between species, to varying environment are good candidates for recurrent selection. Soft selective sweeps on standing genetic variation (*i.e.*, recurrent selection) were for example found as the main source of positive divergent selection in songbirds (Manthey *et al.*, 2021). Some of the regions identified under recurrent selection in *C. arcania* and *C. gardetta* may be under positive selection within and divergent selection between species, which, associated with genetic hitchhiking, can result in genomic blocks of strong differentiation (Charlesworth & Campos, 2014). A more thorough genomic study at the intraspecific level would be necessary to confirm if some of the putative speciation genes identified below could be involved in local adaptation within one or the two species.

The evolutionary processes underlying the formation of genomic barriers

Our results show that 6.6% of the genome would be acting as barrier to gene flow between *C. arcania* and *C. gardetta*. This is three times more than what was found in a pair of

hybridizing *Heliconius* butterflies by Laetsch and colleagues (2023), who show that many loci of weak effect, in addition to 25 strong effect loci, were contributing to reproductive isolation. Another recent study also suggests that reproductive isolation, even in the case of sympatric speciation, could be more polygenic than anticipated (Kautt *et al.*, 2020). The barriers identified between the *Coenonympha* species pair host at least 832 protein-coding genes, and many intergenic regions that could also harbor important regulatory regions. While the exact contribution of each genomic region to reproductive isolation (*i.e.*, their effect sizes) is unknown, it still supports a polygenic nature of reproductive isolation in this case as well.

The vast majority of the barriers identified on the autosomes (92.5% of the 291 autosomal barriers) did not show signals of directional positive selection. Resistance to gene flow between *C. arcania* and *C. gardetta* could then be largely driven by non-adaptive processes, suggesting an important contribution of endogenous barriers to the evolution of reproductive isolation in this species pair. Given that the first 1.5 Myrs of the speciation process was likely realized in strong isolation between the diverging lineages, we can hypothesize that many genes and/or regulatory regions accumulated independent mutations in *C. arcania* and *C. gardetta* genomes. This is supported by the very high genetic differentiation observed on average between the two species. The recombination of co-evolved alleles in hybrids is very often associated with negative interactions, leading to reduced hybrid fitness and increased isolation between the diverging lineages (Coyne, 1992). These endogenous barriers could have arisen as a major driver of reproductive isolation between *C. arcania* and *C. gardetta* during the initial stage of their divergence, while they were not exchanging genetic material. However, adaptive signals were still found in a small proportion of the autosomal barriers, suggesting some influence of exogeneous barriers in the evolution of reproductive isolation. Because selection was supposedly already acting on these genomic regions before the

divergence (*i.e.*, recurrent selection), we can hypothesize that local adaptations in the ancestral population are now differentiating the two species and participate to their reproductive isolation. That would fit well with the strong ecological divergence observed between *C. arcania* and *C. gardetta*, and the identification of many genes involved in adaptation to hypoxia in the barriers showing signals of positive selection. Selection against hybrids would then be partially linked to environmental filtering of unfit phenotypes, reinforcing post-zygotic isolation between the two species. Still on the autosomes, many windows subject to positive selection were found in genomic regions permeable to gene flow (56 windows outside barriers and 22 inside), confirming the potential of our framework to differentiate positive selection contributing or not to reproductive isolation (Laetsch *et al.*, 2023).

The case of the Z chromosome is striking but also delicate to interpret. We identified the Z chromosome as homogeneously resistant to gene flow, supporting that the Z chromosome is a large endogenous and/or exogeneous barrier to reproduction between *C. arcania* and *C. gardetta*. Unlike on the autosomes, the patterns of genetic diversity and differentiation were not contrasted enough on the Z chromosome to easily differentiate the influence of adaptive and non-adaptive processes on shaping the genomic landscape. The proportion of genes with positive DoS (40%) is relatively important on the Z chromosome but most genes still return negative DoS values, indicating that both positive and purifying selection are at play. We also did not find any molecular pathway particularly enriched on the Z chromosome or known important adaptive genes. An entire chromosome the size of the Z chromosome (25.8 Mbp) responding homogeneously to positive selection is also rather unlikely. In that regard, the accumulation of intrinsic non-adaptive genetic incompatibilities could appear as the most likely contributor of reproductive isolation on the Z chromosome as well. Overall, an important role of intrinsic genetic incompatibilities in *C. arcania* and *C. gardetta*

490 reproductive isolation agrees with the results of experimental interspecific crosses that found
491 that F1 hybrids were mostly sterile or very unfit (de Lesse, 1960).

492 *A large Z-effect probably at play in Coenonympha*

493 Sex chromosomes are known to play an exacerbated role in the divergence of many sexual
494 organisms (Presgraves, 2018) and Lepidoptera in particular (Sperling, 1994). A "large X(or
495 Z)-effect" correspond to an exacerbated divergence of the X (or Z) chromosome produced by
496 selection against unfit or sterile hybrids (Coyne, 1992). It assumes the accumulation of
497 incompatible alleles and the involvement of the sex chromosomes in post-zygotic barriers to
498 gene flow between diverging populations or species (Presgraves, 2002). Our results support
499 that a large Z-effect is at play in the divergence process of *C. arcania* and *C. gardetta*. First,
500 we found the almost entire Z chromosome acting as a barrier between *C. arcania* and *C.*
501 *gardetta*, confirming its preponderant role in the evolution of reproductive isolation. Second,
502 we found extreme differences in genomic diversity and differentiation between the autosomes
503 and the Z chromosome, which can indicate an exacerbated influence of the sex chromosomes
504 (Presgraves, 2018; Battey, 2020). The ratio $F_{ST(Z)} / F_{ST(A)} = 1.92$ is much higher in the studied
505 *Coenonympha* species than for most butterfly species pairs (1.44) (Presgraves, 2018). On the
506 contrary, the $\pi_{(Z)}/\pi_{(A)}$ is extremely low for both *C. arcania* (0.51) and *C. gardetta* (0.44). The
507 effective population size of the Z chromosome is ¾ of the one of an autosome, leading to a
508 theoretical diversity ratio of $\pi_{(Z)}/\pi_{(A)} \sim 0.75$ (Charlesworth, 2001), much higher than the one
509 we observed. Unbalanced fertility between sex and/or age classes can lower down this ratio
510 but theory predicts that values below 0.64 would most likely imply the involvement of
511 selection (Charlesworth, 2001). Recent bottlenecks can also influence the $\pi_{(Z)}/\pi_{(A)}$ ratio (Pool
512 & Nielsen, 2007) but we inferred very large effective population sizes for both species,
513 making a recent and strong bottleneck unlikely as the driver of reduced diversity on the Z
514 chromosome.

Adaptive genes between C. arcania and C. gardetta

In the barriers under positive selection, we identified multiple genes potentially associated with response to hypoxia and other stresses. Those would be consistent with the hypothesis of adaptation to high altitude in *C. gardetta,* which involves adapting to lower oxygen pressures and more frequent stresses. For example, the serine/threonine protein kinase, coded by a gene on chromosome 21, is suggested to be linked to activation of mitochondrial respiration in response to a decrease in ATP levels, which happens after a stress and particularly during hypoxia (Murray, 2009). We also found one gene coding for an apoptosis-inducing factor on chromosome 9. Apoptosis-inducing factors are known to be involved in adaptation to high elevation in humans (Sharma *et al.*, 2022) and mammals (Wu *et al.*, 2020), due to their role in regulating apoptosis of the cells during hypoxia. In the same lines, two phosphatidylserine synthases, which act as recognition receptor in apoptotic cells (Naeini *et al.*, 2020) were annotated on chromosome 3, in one of the most interesting genomic barriers. Furthermore, one gene producing a fatty acid synthetase was found on chromosome 15, and a reduced oxidation of fatty acids is suggested to be beneficial at high elevation when hypoxia makes oxidation of carbohydrates more favorable (Ge *et al.*, 2012). Those genes are located on various autosomes and the Z chromosome, suggesting that such adaptation to elevation in *C. gardetta* would be polygenic. The barrier loci also host genes involved in cell functioning, organism development and DNA or RNA repair and expression. Although there is no certainty about the implication of these genes in the speciation process, they might be involved in genomic incompatibilities at the developmental stage or hybrid infertility (Palopoli & Wu, 1994), which would explain the lack of backcrossed individuals found in the field even though F1 hybrids are present. The usual suspects such as *cortex*, *optix* or *WntA*, which are genes classically involved in butterfly speciation (Van Belleghem *et al.*, 2021), were found nowhere near our identified genomic barriers to gene flow. That could suggest a

weak role of wing coloration, patterning and shape in the isolation of this species pair, contrary to many other examples of tropical and temperate butterflies (Jiggins, 2006; Mavárez *et al.*, 2006; Salazar *et al.*, 2010). Important regulatory regions or structural variants could be involved as well in the reproductive isolation between *C. arcania* and *C. gardetta*. Improving our understanding of the *Coenonympha* genome and its functional annotation in the coming years will be an important step to look beyond the genes and integrate more complex genetic features likely involved in the speciation process.

MATERIALS & METHODS

Genomic data acquisition

Nineteen individuals of *Coenonympha arcania* and 17 individuals of *C. gardetta* were sampled across the two species ranges in Europe, with a particular focus on the Alps and their surroundings (Supplemental Table S2). The body of each individual was stored in 90% alcohol and kept at -20 °C until processing. Whole genomic DNA was extracted in the lab from the thorax of each sample using the Qiagen DNeasy blood and tissue kit. Extracted DNA was sent to the Genotoul platform (https://www.genotoul.fr) for whole genome sequencing library preparation using the TruSeq Nano DNA Illumina's Library Preparation kit. The 37 libraries were then sequenced on a lane of Illumina NovaSeq 6000 S4 to generate paired-end 150-bp reads. Read sequences were demultiplexed, clipped of Illumina adapter sequences, and trimmed of low quality flanking sequence (Q<20) using a sliding window of 6 bp using Trimmomatic (Bolger *et al.*, 2014). Mapping of the sequence reads was performed with the program BWA (Li & Durbin, 2009), using the BWA-MEM algorithm. As a reference, we used the new BST1 assembly of *C. arcania* genome described in (Legeai *et al.*, 2024). The SAM files resulting from the aligned reads were converted to BAM files using SAMtools (Li *et al.*, 2009). PCR duplicates were removed using the "*markdup*" function in

564 sambamba-0.6.8 (Tarasov *et al.*, 2017). The filtered BAM files were sorted and indexed
565 using SAMtools.

566 We used ANGSD (Analysis of Next Generation Sequencing Data) (Korneliussen *et*
567 *al.*, 2014), to produce genotype likelihoods for each individual and covered genomic site.
568 ANGSD was first ran independently for each species using the SAMtools genotype
569 likelihood model, only using reads having unique best hits, setting a minimum MapQ score to
570 keep a read to 20, a min nucleotide Q score to consider a site to 20, a minimum number of 5
571 individuals with coverage to consider a site, a minimum of 3 and maximum of 60 reads to
572 estimate genotype likelihood for one individual, keeping only biallelic sites, performing the
573 base alignment quality (BAQ: Phred-scaled probability of a read base being misaligned)(Li,
574 2011) as in SAMtools. We then identified the genomic sites (monomorphic and polymorphic)
575 that were covered for both species and re-ran ANGSD with all samples using the "-site"
576 option to produce a global dataset. For downstream analyses, we either directly used the
577 genotype likelihoods or "hard called" genotypes using a posterior probability cutoff of 80%
578 (more details in Supplemental Code S1).

579 *Inference of historic population dynamics and species divergence*

580 A Site Frequency Spectrum (SFS) was inferred and optimized for each species from the
581 genotype likelihoods using the realSFS sub-program of ANGSD. A total sequence length of
582 203 Mb was used for creating the SFS, including monomorphic and polymorphic sites, all
583 covered in both species. We used Fastsimcoal2 (Excoffier *et al.*, 2013) to compare the
584 likelihood of different speciation scenarios, including strict isolation (SI), isolation with
585 migration (IM), secondary contact (SC) and ancient migration (AM). To avoid making the
586 models overly complex, we modeled gene flow as homogeneous along the genomes and both
587 gene flow and N_e as homogeneous through time for a specific period. These models were
588 compared running 30 independent maximizations of the likelihood based on the observed

589 joint SFS derived from the two species SFS, and retaining the run/model with the lowest
590 AIC. Once the most likely scenario was identified, we estimated the timing of divergence
591 (T_{split}), the timing of gene flow ($T_{gene\text{-}flow}$), the current populations sizes ($N_{arcania}$, $N_{gardetta}$), and
592 the migration rate between species ($m_{arcania\text{-}gardetta}$, $m_{gardetta\text{-}\ arcania}$). These parameters were
593 estimated running 30 independent maximizations of the likelihood based on the observed
594 joint SFS derived from the two species SFS, and retaining the estimate with the highest
595 likelihood. We then performed 100 parametric bootstraps to obtain the 95% confidence
596 interval for each parameter estimate.

597 In parallel, we used the procedure implemented in DILS (Fraïsse *et al.*, 2021) to
598 compare the same divergence models with an ABC framework. DILS was run on 9,840 sets
599 of sequences representing the genotype data for the 36 samples on 20 kbp long genomic
600 windows along the entire reference genome. For a random selection of 1000 sequences, DILS
601 first conducts a genome-wide analysis using an ABC procedure based on random forest and a
602 large set of summary statistics. This first step of the procedure identifies the genome-wide
603 model, and associated parameters, that reproduce best the observed dataset. We checked the
604 validity of the procedure using goodness-of-fit tests (Supplemental Table S3 and Fig. S4).
605 Genetic data were simulated under the best supported model, using the estimated parameters.
606 These simulations then empirically produce the statistical distributions summarized under the
607 inferred model. We then examine whether the value observed from the *Coenonympha* dataset
608 is correctly captured by the inferred model for each of the summary statistics.

609 *Locating barrier loci in the genomes*

610 To look for barrier loci between *C. arcania* and *C. gardetta*, we tested a local reduction of
611 gene flow along the genome using an adaptation of the model-based approach developed in
612 gIMble (Laetsch *et al.*, 2023) and the procedure implemented in DILS (Fraïsse *et al.*, 2021).
613 We had to modify the available version of gIMble because it assumes an isolation with

migration scenario between the diverging populations when the most likely scenario of speciation for *C. arcania* and *C. gardetta* was a secondary contact after a period of strict isolation (see Results). Otherwise, we followed a similar procedure, which tests if the migration rate estimated for a specific genomic region ($m_{e,i}$) is reduced compared to the migration rate inferred for the entire genome (m_e), using coalescent modeling. In our case, the likelihood of a secondary contact (SC) model was compared to a model of strict isolation (SI) for each genomic region of interest. In the first model of divergence, $m_{e,i}$ is fixed to m_e, the divergence time (T_{split}) and the timing of secondary contact (T_{sc}) are also fixed to their genome-wide estimates and only the effective population sizes $N_{arcania}$ and $N_{gardetta}$ are inferred to account for heterogeneity in genetic diversity along the genome. In the second model m_e is fixed to 0 (SI) while $N_{arcania}$ and $N_{gardetta}$ are inferred, and divergence time (T_{split}) is fixed to its genome-wide estimates. Finally, the difference in likelihood (Δ_B) between the two models is estimated to determine if having $m_{e,i} = 0$ improves the fit of the model to the data. The genomic regions for which $\Delta_B > 0$ show a reduced local migration rate compared to the genome-wide estimate and can be considered as putatively involved in reproductive isolation. To apply that procedure on our data, we first used realSFS to estimate and optimize a local 2D-SFS between *C. arcania* and *C. gardetta* for each 50kb genomic window described above. We then used Fastsimcoal2 (Excoffier *et al.*, 2013) to estimate, for each window, the likelihood and parameters of the two models described above. We estimated Δ_B for each genomic window and qualified a region as barrier to gene flow when $\Delta_B > 0$. To account for a possible difference in migration rates between sex chromosomes and autosomes we re-ran the procedure independently for the Z chromosome, using an overall migration rate estimated with this chromosome only. However, if the Z chromosome hosted many barriers, this Z focused procedure would lead to underestimating the real migration rate and therefore the number of barriers on this chromosome. We acknowledge that this is rather circular and

639 unfortunately impossible to resolve precisely without knowing the nature and frequency of
640 migration events between species. Finally, uncertainty in the procedure was quantified by
641 estimating a false positive rate (FPR) for each window. We simulated 100 replicates under
642 the locally best fitting set of N estimates but fixing m_e to $m\square_e$ and T_{split} to the time estimate
643 found with the global model. We then used the same procedure as above to measure the
644 fraction of the simulation replicates for which $\Delta B > 0$.

645 We compared the Δ_B results to the outputs of DILS, which, in addition to inferring
646 demographic parameters, look for barrier loci in the genomes (Fraïsse *et al.*, 2021). DILS was
647 executed with the same input file that was described in the "*demographic inferences*" section.
648 The random forest-based ABC procedure was conducted on each genomic window
649 independently to decide between a scenario of divergence with secondary contact (SC) and a
650 scenario of strict isolation (SI) at the 50kb window level, while accounting for potential
651 variation in effective population size across genomic regions. The mode "*bimodal"* was used
652 (two categories of locus in the genome: proportion *P* linked to barriers with migration rate of
653 zero, 1-*P* not linked to barriers with non-null migration) and we used a mutation rate of
654 2.9×10^{-9} for the simulations. Windows returning a SI posterior probability > 0.7 were
655 considered as barrier loci.

656 *Species genomic diversity along the genome*

657 To characterize patterns of genetic diversity along BST1 reference genome for the two
658 species, we first estimated two population-specific parameters with Tajima's *D* (Tajima,
659 1989) and pairwise nucleotide diversity (π). We measured these parameters for each species
660 independently using the same filtering options, as described above. Pairwise diversity (π) and
661 Tajima's *D* were calculated on abutting genomic windows of 50kb using the realSFS
662 subprogram of ANGSD and its function "*thetaStat*" (Korneliussen *et al.*, 2013) from the
663 species-specific genotype likelihood files. To look at the heterogeneity of genetic divergence

along the genome of the two species, we estimated d_{xy}, the absolute genetic divergence, d_a, the net genetic divergence, and F_{ST}, as a proxy of genetic differentiation, using the same 50kb abutting genomic windows as for the species-specific parameters described above. d_{xy} was estimated following Toews et al. (2016). For each polymorphic site we measured the probability of sampling different alleles between the two species using the species-specific ANGSD allele frequency files (.mafs files) and the formula: $d_{XY} = f_1 * (1 - f_2) + f_2 * (1 - f_1)$, where f_1 is the minor allele frequency in species 1 and f_2 is the minor allele frequency in species 2. The site-specific estimates obtained were then averaged within each genomic window, including monomorphic sites as 0s. Net divergence d_a was estimated for each genomic window as follow: $d_a = d_{XY} - \frac{(\pi_{arcania} + \pi_{gardetta})}{2}$. Mean pairwise F_{ST} values were also estimated for each window from the optimized SFS produced for each species as described above and using the function "*fst*" of the realSFS program. Pairwise LD was estimated using the program ngsLD (Fox *et al.*, 2019), restricting comparisons to pairs of polymorphic sites within each window of 50 kb used above for the estimation of the genetic diversity parameters. LD decay was estimated for each genomic window by weighting the r^2 of the correlation between loci by their physical distance (bp) along the genome. The averaged value was recorded for each window and used as a proxy of linkage strength along the genome.

Direction of Selection (DoS)

We used SNPeff (Cingolani *et al.*, 2012) and the positions along the *BST1* reference genome to annotate the variants to functional classes: upstream and downstream of genes, introns, synonymous, nonsynonymous, intronic, or intergenic sites. We then used this information and the frequency of the different alleles within *C. arcania* and *C. gardetta* populations to estimate, for all protein-coding genes, the direction of selection (DoS) statistics proposed in

(Stoletzki & Eyre-Walker, 2011). This metric results from the adaptation of the McDonald-Kreitmand (MK) test for selection (McDonald & Kreitman, 1991), where the number of synonymous and nonsynonymous substitution (D_n and D_s) are compared to the number of synonymous and nonsynonymous polymorphisms (P_n and P_s). The direction of selection is estimated as follows: DoS = $D_n / (D_n + D_s) - P_n / (P_n + P_s)$, with DoS > 0 suggesting positive selection and DoS < 0 suggesting purifying selection on deleterious mutations (Stoletzki & Eyre-Walker, 2011). In our case D_n and D_s were mutations with divergently fixed alleles in *C. arcania* and *C. gardetta* populations when P_n and P_s represented mutations that were polymorphic in one or the two species.

Signals of selection along the genomes

To locate genomic windows under selection we followed the "correlation of genomic landscapes" approach proposed in Shang et al. (2021) and adapted form Han et al. (2017) and Irwin et al. (2018), which differentiates four evolutionary scenarios based on extremeness of genomic parameters. Each scenario corresponds to specific divergence and selection history with each history being characterized by different patterns of genetic differentiation (F_{ST}), net divergence (d_{XY}) and nucleotide diversity (π). Divergence with gene flow, when selection acts only at specific genes involved in reproductive isolation while gene flow is pervasive elsewhere in the genome, results in high F_{ST}, high d_{XY} and low π. Allopatric selection, when selection acts independently within the two isolated species, results in high F_{ST}, average d_{XY} and low π. Recurrent selection, which relates to similar selective pressure in the two diverging lineages and their ancestral population, results in high F_{ST}, low d_{XY} and low π. Balancing selection, where ancestral polymorphism is maintained by selection, results in low F_{ST}, high d_{XY} and high π. We considered the parameters as being "low" or "high" when they were in bottom or top 5% of the distribution, respectively, and "average" when they fell

between the 30st and 70st percentiles. This characterization was conducted independently on the Z chromosome and the autosomes.

Exploration of the candidate genes

Four types of genomic windows were characterized based on their association with a barrier locus ("linked to barrier" or "unlinked to barrier") and if they showed signals of positive selection (divergent, recurrent or allopatric) with the "correlation of genomic landscapes" approach described above ("positive selection" or "no positive selection"). To explore further the potential pathways involved in reproductive isolation between *C. arcania* and *C. gardetta* we then looked at the genes located in these four types of genomic regions. To assess if these lists of annotated genes were overrepresented for different molecular functions or biological processes, we conducted for each group of windows a gene ontology (GO) term enrichment analysis using the *topGO* R-package (Alexa & Rahnenfuhrer, 2023) and tested the significance of the enrichment using a Kolmogorov Smirnov test. Finally, we exhaustively looked at the genes located in windows linked to barrier and showing signals of positive selection.

DATA ACCESS

Sequence data generated in this study have been submitted to the NCBI BioProject database (https://www.ncbi.nlm.nih.gov/bioproject/1053281), under accession number PRJNA1053281.

Custom scripts to reproduce the analyses conducted in the study can be found in the Supplemental Code S1 and S2, as well as on Github: https://github.com/Capblancq/Speciation-Coenonympha-butterflies/tree/master/Speciation-genomics-arcania-gardetta

COMPETING INTEREST STATEMENT

The authors declare no conflict of interest.

ACKNOWLEDGEMENTS

This project was supported by the French National Research Agency (ANR-20-CE02-0017). We appreciate the assistance of Jesus Mavarez and Paul Doniol-Valcroze for their contribution to the collecting of material used for the genomic study and of Christelle Fraïsse for interesting discussions on our results.

AUTHOR CONTRIBUTIONS

Laurence Després, Mathieu Joron and Thibaut Capblancq conceived the study and collected the samples. TC carried out the laboratory work, analyzed genomic data with the help of Fabrice Legeai and conducted the statistical analyzes with help from Camille Roux and Frédéric Boyer. TC wrote a first draft of the manuscript and all authors provided critical feedback.

REFERENCES

Alexa A, Rahnenfuhrer J. **2023**. topGO: Enrichment Analysis for Gene Ontology.

April J, Hanner RH, Dion-Côté A-M, Bernatchez L. **2013**. Glacial cycles as an allopatric speciation pump in north-eastern American freshwater fishes. *Molecular Ecology* **22**: 409–422.

Barton NH, Hewitt GM. **1985**. Analysis of hybrid zones. *Annual Review of Ecology and Systematics* **16**: 113–148.

Bateson W. **1909**. Heredity and variation in modern lights. *Darwin and modern science*.

Battey CJ. **2020**. Evidence of linked selection on the Z chromosome of hybridizing hummingbirds*. *Evolution* **74**: 725–739.

Bolger AM, Lohse M, Usadel B. **2014**. Trimmomatic: A flexible trimmer for Illumina sequence data. *Bioinformatics* **30**: 2114–2120.

Capblancq T. **2016**. La spéciation hybride : réflexions générales et exploration d ' un cas d' étude chez des papillons alpins du genre Coenonympha.

Capblancq T, Després L, Rioux D, Mavárez J. **2015**. Hybridization promotes speciation in Coenonympha butterflies. *Molecular Ecology* **24**: 6209–6222.

Capblancq T, Mavárez J, Rioux D, Després L. **2019**. Speciation with gene flow: Evidence from a complex of alpine butterflies (Coenonympha , Satyridae). *Ecology and Evolution* **9**: 6444–6457.

Carlson CS, Thomas DJ, Eberle MA, Swanson JE, Livingston RJ, Rieder MJ, Nickerson DA. **2005**. Genomic regions exhibiting positive selection identified from dense genotype data. *Genome Research* **15**: 1553–1565.

Charlesworth B. **2001**. The effect of life-history and mode of inheritance on neutral genetic variability. *Genetical Research* **77**: 153–166.

Charlesworth B. **2012**. The Effects of Deleterious Mutations on Evolution at Linked Sites. *Genetics* **190**: 5–22.

Charlesworth B, Campos JL. **2014**. The Relations Between Recombination Rate and Patterns of Molecular Variation and Evolution in *Drosophila*. *Annual Review of Genetics* **48**: 383–403.

Charlesworth B, Nordborg M, Charlesworth D. **1997**. The effects of local selection, balanced polymorphism and background selection on equilibrium patterns of genetic diversity in subdivided populations. *Genetical Research* **70**: 155–174.

Cingolani P, Platts A, Wang LL, Coon M, Nguyen T, Wang L, Land SJ, Lu X, Ruden DM. **2012**. A program for annotating and predicting the effects of single nucleotide polymorphisms, SnpEff. *Fly* **6**: 80–92.

Coyne JA. **1992**. Genetics and speciation. *Nature* **355**: 511–515.

Coyne JA, Orr HA. **2004**. *Speciation*. Sinauer associates Sunderland, MA.

Cruickshank TE, Hahn MW. **2014**. Reanalysis suggests that genomic islands of speciation are due to reduced diversity, not reduced gene flow. *Molecular Ecology* **23**: 3133–3157.

De Jode A, Le Moan A, Johannesson K, Faria R, Stankowski S, Westram AM, Butlin RK, Rafajlović M, Fraïsse C. **2023**. Ten years of demographic modelling of divergence and speciation in the sea. *Evolutionary Applications* **16**: 542–559.

de Lesse. **1960**. *Zoologie et Biologie Animale*. Paris.

Dobzhansky T. **1936**. Studies on Hybrid Sterility. II. Localization of Sterility Factors in Drosophila Pseudoobscura Hybrids. *Genetics* **21**: 113–135.

Endler JA. **1977**. *Geographic variation, speciation, and clines*. Princeton University Press.

Excoffier L, Dupanloup I, Huerta-Sánchez E, Sousa VC, Foll M. **2013**. Robust Demographic Inference from Genomic and SNP Data. *PLoS Genetics* **9**.

Feder JL, Egan SP, Nosil P. **2012**. The genomics of speciation-with-gene-flow. *Trends in Genetics* **28**: 342–350.

Fox EA, Wright AE, Fumagalli M, Vieira FG. **2019**. ngsLD: evaluating linkage disequilibrium using genotype likelihoods. *Bioinformatics*: 1–2.

Fraïsse C, Popovic I, Mazoyer C, Spataro B, Delmotte S, Romiguier J, Loire É, Simon A, Galtier N, Duret L, *et al.* 2021. DILS: Demographic inferences with linked selection by using ABC. *Molecular Ecology Resources* **21**: 2629–2644.

Ge R-L, Simonson TS, Cooksey RC, Tanna U, Qin G, Huff CD, Witherspoon DJ, Xing J, Zhengzhong B, Prchal JT, *et al.* 2012. Metabolic insight into mechanisms of high-altitude adaptation in Tibetans. *Molecular Genetics and Metabolism* **106**: 244–247.

Han F, Lamichhaney S, Grant BR, Grant PR, Andersson L, Webster MT. **2017**. Gene flow, ancient polymorphism, and ecological adaptation shape the genomic landscape of divergence among Darwin's finches. *Genome Research* **27**: 1004–1015.

Irwin DE, Milá B, Toews DPL, Brelsford A, Kenyon HL, Porter AN, Grossen C, Delmore KE, Alcaide M, Irwin JH. **2018**. A comparison of genomic islands of differentiation across three young avian species pairs. *Molecular Ecology* **27**: 4839–4855.

Jiggins CD. **2006**. Speciation: Reinforced butterfly speciation. *Heredity* **96**: 107–108.

Kautt AF, Kratochwil CF, Nater A, Machado-Schiaffino G, Olave M, Henning F, Torres-Dowdall J, Härer A, Hulsey CD, Franchini P, *et al.* 2020. Contrasting signatures of genomic divergence during sympatric speciation. *Nature* **588**: 106–111.

Kodandaramaiah U, Wahlberg N. **2009**. Phylogeny and biogeography of Coenonympha butterflies (Nymphalidae: Satyrinae)–patterns of colonization in the Holarctic. *Systematic Entomology* **34**: 315–323.

Korneliussen TS, Albrechtsen A, Nielsen R. **2014**. ANGSD: Analysis of Next Generation Sequencing Data. *BMC Bioinformatics* **15**: 356–368.

Korneliussen TS, Moltke I, Albrechtsen A, Nielsen R. **2013**. Calculation of Tajima's D and other neutrality test statistics from low depth next-generation sequencing data. *BMC Bioinformatics* **14**.

Laetsch DR, Bisschop G, Martin SH, Aeschbacher S, Setter D, Lohse K. **2023**. Demographically explicit scans for barriers to gene flow using gIMble (N Bierne, Ed.). *PLOS Genetics* **19**: e1010999.

Legeai F, Romain S, Capblancq T, Doniol-Valcroze P, Joron M, Lemaitre C, Després L. **2024**. Chromosome-Level Assembly and Annotation of the Pearly Heath *Coenonympha arcania* Butterfly Genome (C Wheat, Ed.). *Genome Biology and Evolution* **16**: evae055.

Levsen ND, Tiffin P, Olson MS. **2012**. Pleistocene Speciation in the Genus Populus (Salicaceae). *Systematic Biology* **61**: 401.

Li H. **2011**. Improving SNP discovery by base alignment quality. *Bioinformatics* **27**: 1157–1158.

Li H, Durbin R. **2009**. Fast and accurate long-read alignment with Burrows-Wheeler transform. *Bioinformatics* **25**: 1754–1760.

Li H, Handsaker B, Wysoker A, Fennell T, Ruan J, Homer N, Marth G, Abecasis G, Durbin R. **2009**. The Sequence Alignment/Map format and SAMtools. *Bioinformatics* **25**: 2078–2079.

Manthey JD, Klicka J, Spellman GM. **2021**. The Genomic Signature of Allopatric Speciation in a Songbird Is Shaped by Genome Architecture (Aves: *Certhia americana*) (K Lohmueller, Ed.). *Genome Biology and Evolution* **13**: evab120.

Martin SH, Dasmahapatra KK, Nadeau NJ, Salazar C, Walters JR, Simpson F, Blaxter M, Manica A, Mallet J, Jiggins CD. **2013**. Genome-wide evidence for speciation with gene flow in *Heliconius* butterflies. *Genome Research* **23**: 1817–1828.

Martin SH, Eriksson A, Kozak KM, Manica A, Jiggins CD. **2015**. *Speciation in Heliconius Butterflies: Minimal Contact Followed by Millions of Generations of Hybridisation*. Evolutionary Biology.

Mavárez J, Salazar CA, Bermingham E, Salcedo C, Jiggins CD, Linares M. **2006**. Speciation by hybridization in Heliconius butterflies. *Nature* **441**: 868–871.

McDonald J H, Kreitman M. **1991**. Adaptive protein evolution at the Adh locusin Drosophila. *Nature* **351**: 652–654.

Moreira LR, Klicka J, Smith BT. **2023**. Demography and linked selection interact to shape the genomic landscape of codistributed woodpeckers during the Ice Age. *Molecular Ecology* **32**: 1739–1759.

Muller HJ. **1942**. Isolating mechanisms, evolution, and temperature. In: Biol. Symp. 71.

Murray AJ. **2009**. Metabolic adaptation of skeletal muscle to high altitude hypoxia: how new technologies could resolve the controversies. *Genome Medicine* **1**: 117.

Naeini MB, Bianconi V, Pirro M, Sahebkar A. **2020**. The role of phosphatidylserine recognition receptors in multiple biological functions. *Cellular & Molecular Biology Letters* **25**: 23.

Nevado B, Contreras-Ortiz N, Hughes C, Filatov DA. **2018**. Pleistocene glacial cycles drive isolation, gene flow and speciation in the high-elevation Andes. *New Phytologist* **219**: 779–793.

Noor MAF, Bennett SM. **2009**. Islands of speciation or mirages in the desert? Examining the role of restricted recombination in maintaining species. *Heredity* **103**: 439–444.

Nosil P. **2012**. *Ecological Speciation*. Oxford Univiversity Press.

Nosil P, Funk DJ, Ortiz-Barrientos D. **2009**. Divergent selection and heterogeneous genomic divergence. *Molecular Ecology* **18**: 375–402.

Palopoli MF, Wu C-I. 1994. Genetics of Hybrid Male Sterility Between Drosophila Sibling Species: A Complex Web of Epistasis Is Revealed in Interspecific Studies. *Genetics*: 329–341.

Pool JE, Nielsen R. 2007. POPULATION SIZE CHANGES RESHAPE GENOMIC PATTERNS OF DIVERSITY. *Evolution* **61**: 3001–3006.

Presgraves DC. 2002. PATTERNS OF POSTZYGOTIC ISOLATION IN LEPIDOPTERA. *Evolution* **56**: 1168–1183.

Presgraves DC. 2010. The molecular evolutionary basis of species formation. *Nature Reviews Genetics* **11**: 175–180.

Presgraves DC. 2018. Evaluating genomic signatures of "the large X-effect" during complex speciation. *Molecular Ecology* **27**: 3822–3830.

Ravinet M, Faria R, Butlin RK, Galindo J, Bierne N, Rafajlović M, Noor MAF, Mehlig B, Westram AM. 2017. Interpreting the genomic landscape of speciation: a road map for finding barriers to gene flow. *Journal of Evolutionary Biology* **30**: 1450–1477.

Roux C, Fraïsse C, Romiguier J, Anciaux Y, Galtier N, Bierne N. 2016. Shedding Light on the Grey Zone of Speciation along a Continuum of Genomic Divergence. *PLoS Biology* **14**: 1–23.

Salazar C, Baxter SW, Pardo-Diaz C, Wu G, Surridge A, Linares M, Bermingham E, Jiggins CD. 2010. Genetic Evidence for Hybrid Trait Speciation in Heliconius Butterflies. *PLoS Genetics* **6**: e1000930.

Schluter D. 2009. Evidence for Ecological Speciation and Its Alternative. *Science* **323**: 737–741.

Seehausen O, Butlin RK, Keller I, Wagner CE, Boughman JW, Hohenlohe PA, Peichel CL, Saetre G-P, Bank C, Brännström Å, *et al.* 2014. Genomics and the origin of species. *Nature Reviews Genetics* **15**: 176–192.

Shang H, Rendón-Anaya M, Paun O, Field DL, Hess J, Vogl C, Liu J, Ingvarsson PK, Lexer C, Leroy T. 2021. *Drivers of genomic landscapes of differentiation across* Populus *divergence gradient*. Evolutionary Biology.

Sharma V, Varshney R, Sethy NK. 2022. Human adaptation to high altitude: a review of convergence between genomic and proteomic signatures. *Human Genomics* **16**: 21.

Simon A, Bierne N, Welch JJ. 2018. Coadapted genomes and selection on hybrids: Fisher's geometric model explains a variety of empirical patterns. *Evolution Letters* **2**: 472–498.

Smadja CM, Butlin RK. 2011. A framework for comparing processes of speciation in the presence of gene flow: FRAMEWORK FOR COMPARING PROCESSES OF SPECIATION. *Molecular Ecology* **20**: 5123–5140.

Sperling FAH. 1994. SEX-LINKED GENES AND SPECIES DIFFERENCES IN LEPIDOPTERA. *The Canadian Entomologist* **126**: 807–818.

Stankowski S, Ravinet M. **2021**. Defining the speciation continuum. *Evolution* **75**: 1256–1273.

Stoletzki N, Eyre-Walker A. **2011**. Estimation of the Neutrality Index. *Molecular Biology and Evolution* **28**: 63–70.

Tajima F. **1989**. Statistical Method for Testing the Neutral Mutation Hypothesis by DNA Polymorphism. *Genetics Society of America*: 585–595.

Tarasov A, Vilella AJ, Cuppen E, Nijman IJ, Prins P. **2017**. Genome analysis Sambamba□: fast processing of NGS alignment formats. *Bioinformatics* **31**: 2032–2034.

Toews DPL, Taylor SA, Vallender R, Brelsford A, Butcher BG, Messer PW, Lovette IJ. **2016**. Plumage Genes and Little Else Distinguish the Genomes of Hybridizing Warblers. *Current Biology* **26**: 2313–2318.

Turner TL, Hahn MW, Nuzhdin SV. **2005**. Genomic Islands of Speciation in Anopheles gambiae (N Barton, Ed.). *PLoS Biology* **3**: e285.

Van Belleghem SM, Cole JM, Montejo□Kovacevich G, Bacquet CN, McMillan WO, Papa R, Counterman BA. **2021**. Selection and isolation define a heterogeneous divergence landscape between hybridizing *Heliconius* butterflies. *Evolution* **75**: 2251–2268.

Wu D-D, Yang C-P, Wang M-S, Dong K-Z, Yan D-W, Hao Z-Q, Fan S-Q, Chu S-Z, Shen Q-S, Jiang L-P, *et al.* 2020. Convergent genomic signatures of high-altitude adaptation among domestic mammals. *National Science Review* **7**: 952–963.